

# Development of an elastomer coated hip prosthesis

S. V. JAECQUES\*, J. A. HELSEN

*K. U. Leuven, Department of Metallurgy and Materials Engineering, de Croylaan 2, B-3001 Leuven, Belgium*

J. P. SIMON

*K. U. Leuven, Orthopaedic Hospital, Weligerveld 1, B-3212 Pellenberg, Belgium*

D. MATTHEEUWS

*R. U. Gent, Faculty Veterinary Medicine, Casinoplein 24, B-9000 Gent, Belgium*

A cementless stem for a total hip replacement (THR) was designed aiming at some mechanical advantages of a cemented stem. It is called elastomer coated prosthesis (ECP) and has a metal core, coated with an elastomer layer as a mechanical buffer between the core and the femoral cortex. For the ECP coating a thermoplastic polyolefin elastomer (TPO) was chosen. Required implant sizes were determined from a measurement campaign on the intramedullar canal of German Shepherds' femora. Stress distribution in photo-elastic models of the ensemble ECP core and TPO coating was studied and compared to a model of a cementless system. The core was tested for fatigue resistance in a simulator.

Extensive *in vitro* testing of all ECP components (both core and elastomer coating) has shown that the prosthesis is mechanically suitable for its application. Animal testing was limited to a strict minimum for ethical reasons. Only after obtaining sufficient evidence for biocompatibility *in vitro*, the elastomer was studied *in vivo*. Implantation of non-loaded TPO samples in dogs has shown acceptable behaviour in contact with bone and marrow. ECP prototypes are currently being implanted in German Shepherds and post mortem histology will have to deliver final proof of this concept's validity.

## 1. Introduction

In the field of total hip replacement (THR), a dichotomy exists between cemented and cementless fixation of the femoral stem. While a mantle of polymethyl-metacrylate (PMMA) bone cement has disadvantages, listed in the 'side-effects' section of the instruction leaflet of any commercially available PMMA bone cement, it has the advantage of being a mechanical buffer between prosthesis and bone. This prevents to some extent the stress shielding which is a major drawback of many cementless designs. Therefore, a design was developed with the mechanical advantages of a cemented THR stem but without the use of cement. It was called elastomer coated prosthesis (ECP) and has a metal core that is coated with an elastomer layer as a mechanical buffer between the core and the cortical bone of the femur. The rationale for this choice is the following: impacts from cyclic loading during walking or jumping are dampened by the elastomer. The relatively low hardness of the elastomer layer (80 Shore A) and its elasticity facilitate a press fit fixation in the medullar cavity and decrease the risk of longitudinal femoral fracture at implantation. Point contacts between bone and ECP stem are

spread out into area contacts, greatly reducing local stress concentrations. This also allows some latitude in the reaming process as small irregularities and misfits can be smoothed out by the deformation of the elastomer. Micromovements between ECP stem and bone should be attenuated by a shearing deformation of the elastomer layer and this should eliminate relative movement at the interfaces bone/elastomer and elastomer/ECP core. Generation of wear particles would then be significantly reduced, and metal debris from wear of the core or metal ions from corrosion processes [1] should be contained within the elastomer mantle, avoiding contamination of the surrounding tissue. Metallosis of tissue surrounding titanium implants in particular is now a well-documented phenomenon [2].

For the elastomer layer, a thermoplastic polyolefin elastomer (TPO) was chosen and submitted to an in-depth fatigue and biocompatibility study. Mechanical resistance to fatigue was tested with a simulator. Loads in the human physiologic range were applied for up to  $25 \cdot 10^6$  cycles. A wide array of techniques was used to assess damage: microscopy (optical and scanning electron microscopy (SEM), wide and small angle

\* To whom correspondence should be addressed.

X-ray scattering (WAXS and SAXS), small angle neutron scattering (SANS), dynamic mechanical thermal analysis (DMTA), infrared spectroscopy (FTIR) and swelling. Biocompatibility was certified with the tests for USP Class VI compliance and with *in vitro* tests under more severe conditions. Results of the *in vitro* mechanical testing programme and the *in vitro* biocompatibility testing were satisfactory [3, 4]. The influence of the elastomer coating on the stress distribution in the ECP core and in the surrounding bone was then studied to determine the optimal shape and thickness of the elastomer coating. For the outer shape of the ECP, the design as used in a study by Maistrelli *et al.* [5] was adopted for comparability. Before manufacturing and implanting prototypes, the response to non loaded TPO implants was studied on a small number of dogs and found satisfactory. A measuring campaign on reamed femoral cavities was necessary to determine the required sizes of ECP prototypes to start an *in vivo* study with German Shepherd dogs. This dog breed was chosen because in clinical practice most canine THR's are performed on it [6]. A set of prototypes could then be manufactured and implanted.

## 2. Experimental

### 2.1 Stress distribution

Models of the ensemble of ECP core and TPO coating were examined in a photoelastic study and compared to a model of a conventional cementless implementation of the same system to study the influence of the elastomer coating on the stress distribution in the surrounding bone and to verify that the locally reduced thickness of the ECP core had not introduced dangerous stress concentrations.

Models were machined from 10 mm thick Araldite-B epoxy resin plates and had two components: a rectangular plate in which a frontal section of a femoral cavity had been machined and a frontal section of a prosthesis stem with a 10 mm diameter hole in the centre of the modelled femoral head. Loads were applied in the centre of this hole. The plate was made in two versions, one with only a section of the femoral cavity and another with a 10 mm wide sleeve through the full thickness of the plate on both sides of this section. The remaining 3 mm of epoxy resin modelled a frontal section of the cortex. For the prosthesis stem three models were made: (1) exactly fitting into the cavity (model for a conventional press-fit cementless design), (2) the same shape, but on the outer edge 2 mm was machined away and (3) the same as (2) but with extra resin removed proximo-medially and disto-laterally. In (2) and (3) the open space was filled with a strip of TPO. Two hardnesses of TPO were used: 2-73 and 2-87 (73 and 87 Shore A).

Models were loaded with 200 N in the direction of the resultant force in single leg stance. Bright field isochromate images were observed under circularly polarized monochromatic light ( $\lambda = 589 \text{ nm}$ ) in a Mönch-Ficker projection polariscope [7]. Photographs of the projection screen were transformed to black and white monochrome bitmaps.

### 2.2. In vivo program with non-loaded implants

As a last test before actually manufacturing ECP prototypes, non-loaded implants were inserted in the femoral cortex and medullar cavity of mongrel dogs; undecalcified bone sections were made with the cutting-grinding technique [8].

### 2.3. Determination of required sizes

A measurement programme on the femoral cavities of German Shepherd dogs was necessary since the available literature (e.g. [9–11]) does not contain quantitative data to determine implant sizes for a test population of German Shepherds. Forty-one cadaver femora were used; these were by-products of other institutionally approved animal studies. No animal was killed specifically for this measuring programme. The femora were prepared for insertion of a cementless hip prosthesis by osteotomy of the femoral head and neck and reaming with standard surgical instruments. An imprint of the reamed cavity was made with the IMP system<sup>®</sup> of Stewal Implants<sup>®</sup> (known as "Identifit<sup>®</sup>" in the USA). Data were analysed according to a seven parameter geometric model of the proximal medullar cavity of the canine femur. Detailed results are being published separately [12].

### 2.4. Design and production of prototypes

A first ECP prototype core was then machined from a Ti–Al–Nb alloy according to the drawing in Fig. 1. The distal fixation rod is to be removed before implantation. A collarless design was chosen because the biomechanical advantages of a collar do not seem to compensate the clinical disadvantages when a collar is imperfectly seated [13, 14]. Kwong [15] published a clear review of this topic. Moreover, imperfect contact of collar and calcar will introduce additional variability in the proximal stress transfer [16], making assessment of the elastomer coating's effect more difficult. The coating was to be applied later by injection moulding. Fixation is achieved mechanically: the coating penetrates the core through two sleeves on the centreline. They are filleted in such a way as not to adversely affect the core's fatigue resistance.

### 2.5. Fatigue testing of prototype core

The prototype core of the 12 mm ECP was subjected to fatigue in a geometry causing mainly bending stresses in the stem. A Schenck servohydraulic fatigue tester applied the load. Details should be clear from Fig. 1.

The force amplitude was increased in steps during the test, ending at 2900 N or  $\approx 10$  times the body weight of a 30 kg dog. An overview of the force amplitude versus number of cycles is given in Fig. 2. Frequency of oscillation was 20 Hz. A total number of approx.  $61 \cdot 10^6$  cycles were applied.

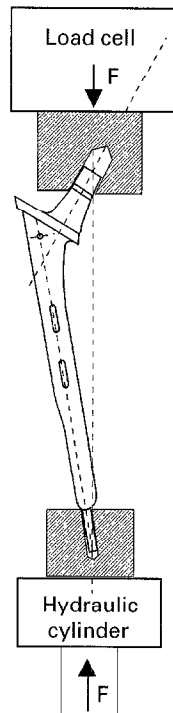


Figure 1 Prototype ECP core mounted in the servohydraulic fatigue tester in a geometry causing mainly bending stresses in the core. The sleeves in the centreline of the core are meant for later mechanical fixation of an elastomer coating.

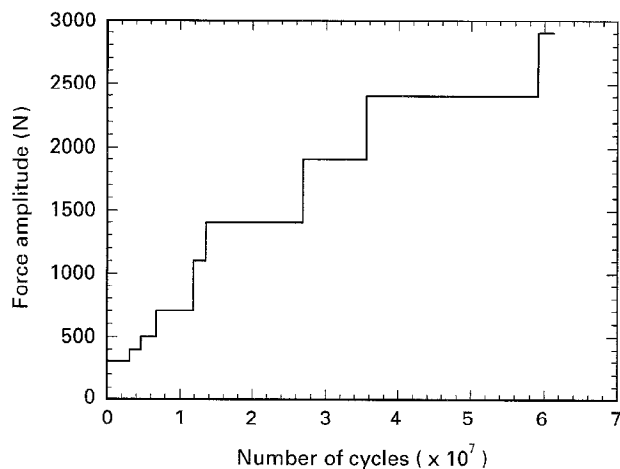


Figure 2 Load amplitudes applied during fatigue of the prototype ECP core.

### 3. Results and discussion

#### 3.1. Stress distribution

Models were checked for initial stresses in unloaded condition (e.g. residual stresses from machining). A limited edge effect was eliminated by annealing for 24 h. After this treatment no stresses were present that could significantly interfere with observations.

In massive plates without sleeves an isochromate image was created upon insertion of the stems; changes upon loading were less pronounced than would be expected. Insertion was difficult due to the stiffness of the femoral cavity model. As this model without sleeves is obviously an oversimplification of reality, no conclusions could be drawn, except for the exactly fitting stem (Fig. 3), where strong stress concentrations were present around the distal tip, prox-

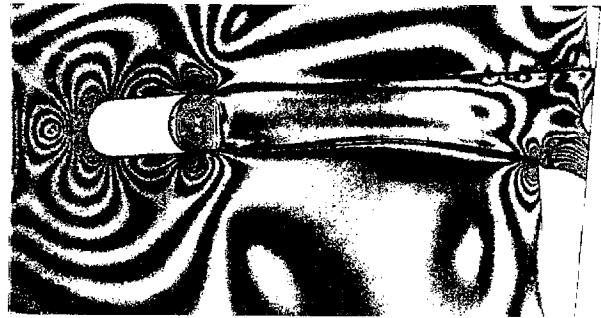


Figure 3 Photo-elastic model of a conventional cementless THR stem inserted in a cavity machined in a massive plate. Load was applied in the direction of resultant force in single leg stance, acting on the centre of the femoral head.

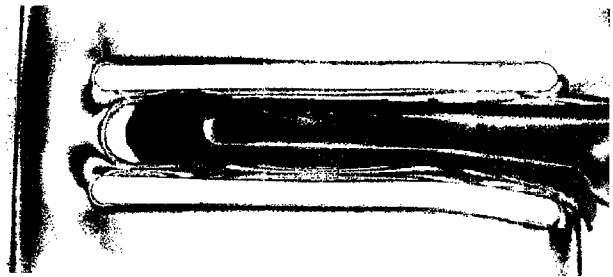


Figure 4 Photo-elastic model of ECP core with TPO 2-73 layer of continuous thickness, not loaded.

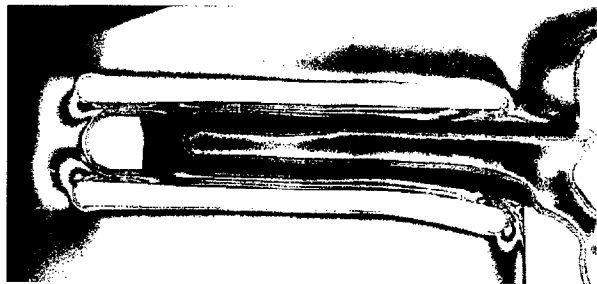


Figure 5 Photo-elastic model of an ECP core with extra thick elastomer coating (2-73) proximo-medially and disto-laterally, not loaded.



Figure 6 Photo-elastic model of ECP core with elastomer coating (2-73) of continuous thickness, loaded with 200 N in the direction of the resultant force in single leg stance, acting on the centre of the femoral head.

imo-medially (calcar region) and proximo-laterally (greater trochanter area). These were attributed to small imperfections in the fit of the stem into the cavity.

In the models with sleeves the clearest isochromate images were observed (Figs 4-7). Under unloaded



Figure 7 Photo-elastic model of ECP core with extra thick elastomer (2-73) coating disto-laterally and proximo-medially, loaded with 200 N in the direction of the resultant force in single leg stance, acting on the centre of the femoral head.

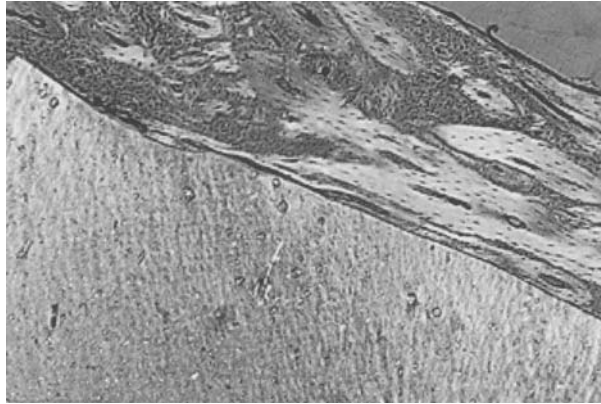


Figure 8 Bone apposition (dark grey) on implant (light grey) after over 11 months implantation. Original magnification  $80\times$ . "Elephant foot" structures can be seen where the bone touches the implant.

conditions the modelled cortex shows parallel isochromates, indicating pure bending, except extremely distal and medial, where a pattern characteristic for compression stress is observed. Upon loading, the isochromate pattern indicates that stress in the modelled cortex decreases medially and increases laterally. Contact between stem and cortex is lost distally and medially.

The stem with extra thick elastomer layer proximo-medially and disto-laterally (Fig. 7) shows less pronounced stress concentrations in the modelled cortex and calcar than the model stem with an elastomer layer of continuous thickness (Fig. 6). No significant difference could be observed between the two hardnesses of TPO. In the stem with extra elastomer (Fig. 7), stresses were higher where core material had been removed to be replaced by elastomer; the highest stresses were however always observed in the model neck. It can be assumed that the shape adaptations to accommodate the elastomer mantle have not introduced dangerous stress concentrations in the stem core.

### 3.2. *In vivo* program with non-loaded implants

Fig. 8 shows a micrograph of a ground PMMA embedded section. The implant was in contact with the femoral cortex for more than 11 months. Staining was done with Stevenel's blue and Van Giesen picrofuch-

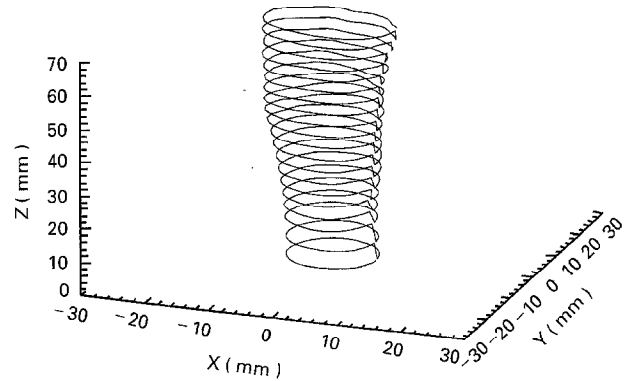


Figure 9 Wire model of the silicone imprint of the reamed proximal femoral cavity of a 35 kg German Shepherd dog.

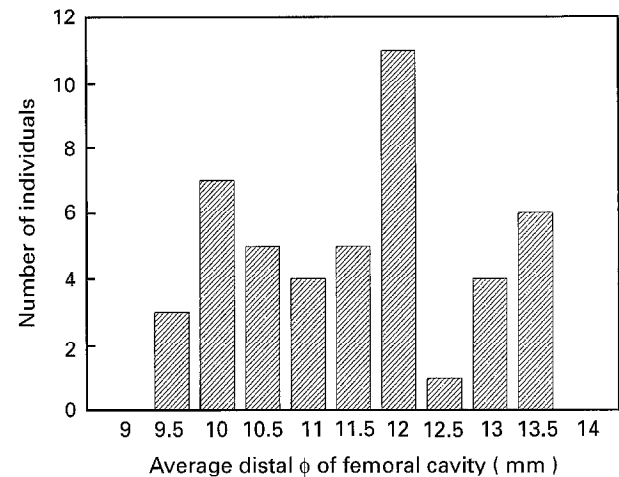


Figure 10 Distribution of the parameter average distal diameter over the examined sample of 41 femora.

sin counterstain. In the micrograph, mature bone is coloured dark grey and the implant is light grey. At the interface bone/implant there is clear bone apposition. However, this can only be achieved if a tight press-fit is realized at implantation; otherwise, fibrous tissue will encapsulate the Sarlink TPO implant.

### 3.3. Determination of required sizes

Results of the measurement programme on cadaveric femora can be seen in Fig. 9 and Fig. 10. From the distribution of the measured distal diameters, it was decided to manufacture the ECP in four sizes, with distal diameters of resp. 10, 11, 12 and 13.5 mm.

### 3.4. Fatigue testing of prototype core

During the fatigue test, force and displacement were recorded. From these data, hysteresis curves and displacement versus number of cycles graphs can be calculated. The hysteresis loops have an area of zero  $\pm$  the accuracy of the machine, i.e. the deformation is completely elastic, even at the highest force level (3000 N). The slope of the hysteresis loops, though not equal to the E-modulus, is a measure for the stiffness of the core and does not change significantly during the test. The average value is  $(7200 \pm 800)$  N/m. Deviations are probably due to

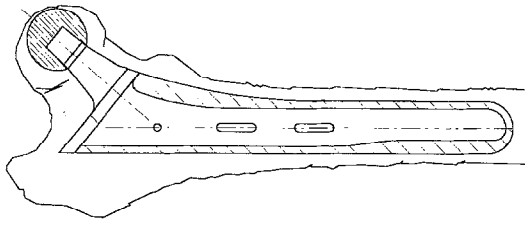


Figure 11 Sectional view of ECP prototype with coating (hatched) shown over an outline of a canine proximal femur.

either fretting wear between the cone and the aluminium fixture or to plastic deformation of the aluminium fixture. Visual evidence of fretting wear was present as a grey-white debris on the base of the cone and on the lower aluminium fixture. The displacement initially increases slightly with increasing number of cycles but apparently has an asymptotic value. This is attributed to plastic deformation and/or fretting at the contact zone of the cone and the aluminium fixture. The present design of the ECP-core has sufficient resistance to mechanical fatigue as applied with our setup, i.e. load levels 100–3000 N, 20 Hz frequency,  $61.10^6$  cycles, atmosphere of 60% humidity and 21 °C.

#### 4. Conclusion

Extensive *in vitro* testing of all components of the ECP (both core and elastomer coating) has shown that the prosthesis is mechanically suitable for its application. The use of test animals has been limited to a strict minimum for ethical reasons. Only after sufficient evidence for biocompatibility was obtained by *in vitro* methods, the elastomer was studied *in vivo*. *In vivo* tests of non-loaded TPO samples have shown acceptable behaviour in contact with bone and marrow tissue of dogs. Elastomer coated prostheses as the one shown in Fig. 11 have been implanted in dogs and post mortem histology will have to deliver final proof of the validity of this concept.

#### Acknowledgements

Grant 910219 from IWONL to S.V.J. is gratefully acknowledged. Stewal Implants is acknowledged for its excellent technical assistance with the preparation and the use of the IMP system for measurement of femoral imprints. Research funded with a specialization scholarship of the Flemish Institute for the en-

couragement of scientific and technological research in industry (IWT).

#### References

1. N. BRUNEEL and J. A. HELSEN, *J. Biomed. Mat. Res.* **22** (1988), 203–214.
2. J.-P. SIMON, in "Restoration of bone stock with impacted cancellous allografts and cement in revision of the femoral component in total hip arthroplasty. A clinical and biomechanical study." PhD Thesis (K. U. LEUVEN, Department of Orthopaedic Surgery, 1994), 207 pp.
3. J. A. HELSEN, S. V. JAECQUES, J. VAN HUMBEECK and J.-P. SIMON, *J. Mater. Science: Materials in Medicine*, **4** (1993) 471–480.
4. J. A. HELSEN, S. V. JAECQUES, J.-P. SIMON and H. DE SMEDT, in Proceedings of the 8th CIMTEC, Firenze, July 1994, edited by P. VINCENZINI (Techna Publ. 1995), Vol. L: Materials in Clinical Applications, X + 812 pp., "In vitro and in vivo compatibility testing of thermoplastic polyolefins", (in press).
5. G. L. MAISTRELLI, V. FORNASSIER, A. BINNINGTON, K. MCKENZIE, V. SESSE and I. HARRINGTON, *J. Bone Joint Surg. [Br.]*, **73-B** (1991) 43–46.
6. M. L. OLMSTEAD, R. B. HOHN and TH. M. TURNER, *J. Am. Vet. Med. Assoc.* **183** (1983) 191–194.
7. L. FÖPPL and E. MÖNCH, in "Praktische Spannungsoptik" (Springer-Verlag, Berlin, 1972), 300 pp.
8. K. DONATH in "Preparation of Histologic Sections by the Cutting-Grinding Technique for Hard Tissue and other material not suitable to be sectioned by routine methods — Equipment and Methodical Performance" (Exakt-Kulzer Publication, Norderstedt 1990), 15 pp.
9. A. CASIOS, J. BOU, M. J. CASTIELLA and C. VILADIU, *J. Morph.* **190** (1986), 73–79.
10. D. R. SUMNER, TH. M. TURNER and J. O. GALANTE, *J. Orthop. Res.* **6** (1988) 758–765.
11. D. R. SUMNER, T. C. DEVLIN, D. WINKELMAN and TH. M. TURNER, *J. Orthop. Res.* **8** (1990) 671–677.
12. S. V. N. JAECQUES, J. A. HELSEN, M. MULIER and D. MATTHEEUWS, Geometric Analysis of the Proximal Medullar Cavity of the Femur in the German Shepherd, submitted to *J. Orthop. Res.* May 1995.
13. K. DJERF and J. GILLQUIST, *Acta. Orthop. Scand.* **58** (1987), 97–103.
14. L. A. WHITESIDE, D. AMADOR and K. RUSSELL, *Clin. Orth. Rel. Res.* **231** (1988) 120–126.
15. K. S. C. KWONG, *J. Bone Joint Surg. [Br.]* **72-B** (1990), 664–665.
16. J. D. BOBYN, A. H. GLASSMAN, H. GOTO, J. J. KRYGIER, J. E. MILLER and E. BROOKS, *Clin. Orth. Rel. Res.* **261** (1990) 196–213.

Received 29 June  
and accepted 4 July 1995